

New methods for measuring macromolecular interactions in solution via static light scattering: basic methodology and application to nonassociating and self-associating proteins

Arun K. Attri¹, Allen P. Minton*

Section on Physical Biochemistry, Laboratory of Biochemistry and Genetics, National Institute of Diabetes and Digestive and Kidney Diseases, National Institutes of Health, U.S. Department of Health and Human Services, Bethesda, MD 20892, USA

Received 25 August 2004

Available online 9 December 2005

Abstract

A method for rapid detection and characterization of reversible associations of macromolecules in solution is presented. A programmable dual-syringe infusion pump is used to introduce a solution of time-varying composition into parallel flow cells for concurrent measurement of laser light scattering at multiple angles and ultraviolet–visible absorbance. An experiment lasting less than 15 min produces a large and information-rich set of data, consisting of several thousand values of the Rayleigh ratio as a function of solute concentration(s) and scattering angle. Using a novel treatment of the data, the entire data set may be equally rapidly analyzed in the context of models for self-association. Validation experiments conducted on previously characterized nonassociating and self-associating proteins yielded robust values for molecular weights in the range 10–330 kDa and equilibrium association constants for dimer formation in the range 2×10^3 – 6×10^5 M⁻¹.

© 2004 Elsevier Inc. All rights reserved.

The detection and characterization of protein–protein interactions in solution is an essential component of overall proteomic strategy [1]. A wide variety of experimental methods are available for the study of such interactions, many of which are reviewed in Phizicky and Fields [1] and Srere [2]. At one end of the spectrum are high-throughput assays for protein–protein interactions, such as the yeast two-hybrid and tandem pull-down assays [3], which provide, at best, qualitative information about strong interactions leading to tightly bound complexes and no information whatsoever about weaker interactions and reversible associations associated with regulatory processes. At the other end of the spectrum are physical–chemical techniques such as sedimentation equilibrium, isothermal titration calorime-

try, and a variety of spectroscopic assays, which can provide quantitative information of high resolution about association equilibria but which are low throughput and labor intensive as conventionally practiced [2]. We present here a novel implementation of one high-resolution technique, light scattering, which greatly accelerates the processes of data acquisition and analysis and increases precision, sensitivity, and range of applicability while substantially decreasing the amount of manual intervention required of the investigator.

The measurement and analysis of static light scattering is a classical technique for determination of molar masses and radii of gyration of synthetic and biological macromolecules in solution. Basic principles underlying the method and the first practical means of performing the required measurements were developed during the 1940s and 1950s [4–7]. The subsequent commercial availability of flow cells for the measurement of light scattering and refractive index made possible the estima-

* Corresponding author. Fax: +1 301 402 0240.

¹ Present address: School of Environmental Sciences, Jawaharlal Nehru University, New Delhi 110 067, India.

tion of molecular weights and radii of gyration of macromolecular solutes in individual peaks eluted from chromatography columns [8,9]; hence permitting rapid detection and identification of stable macromolecular complexes present in solution [10,11]. The composition dependence of the light scattering of a mixture of macromolecules may be analyzed to yield information about attractive and repulsive interactions between individual macromolecule species [7,12,13]. However, acquisition of such information utilizing conventional batch procedures (see for example Tojo et al. [14]) is a time-consuming and labor-intensive process; hence it is rarely utilized. In the present work we demonstrate that a commercially available liquid dispensing instrument can be used in conjunction with flow detectors of light scattering and absorbance to acquire large quantities of accurate composition-dependent light scattering data rapidly and automatically. We additionally demonstrate that with the aid of a new analytical procedure, the data so acquired may be interpreted equally rapidly to yield reliable estimates of the molar mass(es) of macromolecule species and the strength of reversible associations between them.

Methods

Materials

Albumin (bovine serum monomer), albumin (chicken egg white), alcohol dehydrogenase (yeast), cytochrome *c* (horse heart), fibrinogen (bovine plasma, type IV), pepsinogen (porcine stomach), β -lactoglobulin A (bovine milk), β -lactoglobulin B (bovine milk), lysozyme (chicken egg white), and hemoglobin (human) were obtained from Sigma–Aldrich. Chymotrypsinogen A (3 \times crystallized) was obtained from Worthington Chemical. Except for hemoglobin, all proteins were used without further purification. Hemoglobin was converted to cyanmethemoglobin as described in Benesch et al. [15].

Sample preparation

Before use, all protein solutions were extensively dialyzed against phosphate-buffered saline (PBS),² pH 7.2 (Biosource, Biofluids, USA). Hemoglobin solutions prepared in high-ionic-strength buffers were dialyzed against PBS to which the requisite quantity of NaCl was added. Buffers were prefiltered through Millipore 0.22- μ m filters. Protein solutions were prefiltered through 0.02- μ m Whatman Anotop filters. Immediately before experiments were performed, buffers and protein solutions were centrifuged at 1000g for 15 min to

remove residual particulates and microscopic bubbles. All measurements were carried out at 20 °C.

Instrumentation

Solutions dispensed by a Hamilton Microlab 900 dual-syringe precision dispenser (Hamilton, Reno, NV) are delivered through a Whatman Anotop 0.1- μ m filter to a Wyatt DAWN-EOS multiangle laser light scattering detector (Wyatt Technology, Santa Barbara, CA), equipped with a temperature-regulated K5 flow cell and a Milton Roy SM3100 variable-wavelength UV–visible absorbance detector (Thermo Finnegan, West Palm Beach, FL), installed in parallel as indicated schematically in Fig. 1. The analog output of the absorbance detector (1 V per absorbance unit) is connected to the AUX1 input of the DAWN-EOS, and data from the scattering and absorbance detectors are collected simultaneously using ASTRA software (Wyatt Technology; Release 4.90.04). Adjustment of the flow rate in each of the parallel flow paths is necessary to ensure that absorbance measured at a particular time point corresponds to the composition of solution scattering light at the same time point.

Refractive increments of proteins were measured using a thermostatted Leica ARIAS 500 Abbé refractometer (Reichert Instruments, Buffalo, NY) and corrected for differences between the measurement wavelengths of the refractometer (589 nm) and the DAWN-EOS (690 nm) according to Perlmann and Longworth [16]. Extinction coefficients of proteins at the appropriate wavelengths were measured by injection of protein solutions of known concentration into the absorbance detector, and applicability of Beers' Law was confirmed for all proteins examined.

Experimental procedure

A typical experiment is conducted as follows. Following baseline measurement, the dual-syringe dispenser, under program control, provides a stepwise gradient of solute concentration that varies roughly linearly either upward from zero concentration (pure buffer) to the concentration of the stock solution or downward from the concentration of stock solution to zero concentration, over a period of several (typically 5–10) minutes. A single gradient in either direction requires as little as 1 ml of buffer and 1 ml of a stock protein solution with absorbance exceeding 0.1 OD units at the selected wavelength. During this period the relative intensity of light scattered at 15 angles and the absorbance of the sample are collected at regular intervals of time (typically 0.5–1 s). In Fig. 2, the relative intensity of 690-nm light scattered at 90° and the relative absorbance of the solution at 280 nm recorded in a typical experiment are plotted as functions of time. Raw data are saved in native ASTRA format and exported as text files for analysis as described below.

² Abbreviation used: PBS, phosphate-buffered saline.

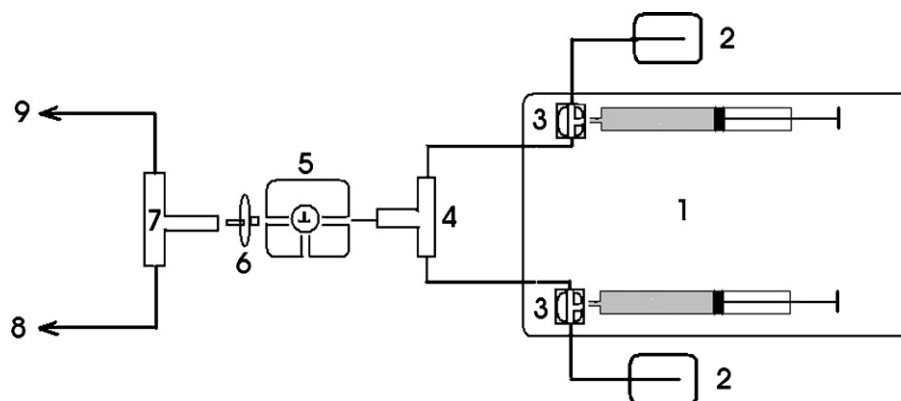


Fig. 1. Schematic view of the liquid handling system. (1) Programmable dual-syringe pump; (2) reservoirs for stock solution and solvent; (3) programmable three-way valves for switching between filling and dispensing modes; (4) stream mixer; (5) three-way valve to facilitate purging/cleaning of the flow system; (6) inline filter; (7) stream splitter; (8, 9) parallel solution delivery lines to flow cells for measurement of light scattering and absorbance.

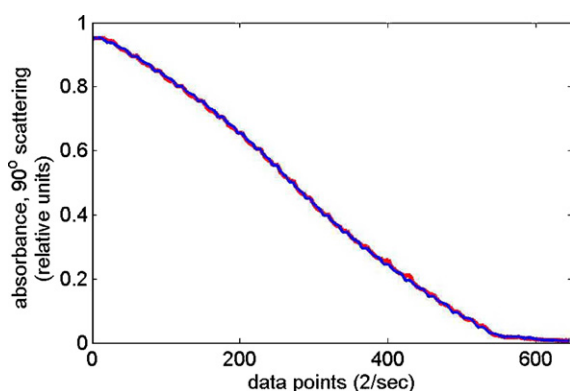


Fig. 2. 90° Light scattering (690 nm, red curve) and absorbance (280 nm, blue curve) of a solution of hen egg ovalbumin, plotted as a function of elapsed time through a dilution gradient and measured as number of collected data points. (For interpretation of the references to color in this figure legend, the reader is referred to the web version of this paper.)

Data analysis

All calculations described below are performed automatically using scripts and functions, written and executed in MATLAB (Mathworks, Natick, MA), that are available upon request.

Using previously measured extinction coefficient(s), absorbance data are converted into time-dependent concentration data and, following procedures provided in the DAWN-EOS instruction manual, the raw scattering data are converted to concentration- and angle-dependent values of the Rayleigh ratio for excess (solute) scattering $R(\theta, \{w\})$, where $\{w\}$ denotes the composition of the solution specified by the weight/volume concentration of all solute species. Additionally, the value of the optical constant K' is calculated according to

$$K' = 4\pi^2 n_o^2 \lambda_o^{-4} N_A^{-1}, \quad (1)$$

where n_o denotes the refractive index of buffer, λ_o is the wavelength in vacuum of the scattering light (690 nm), and N_A is Avogadro's number. The value of the Rayleigh ratio R at zero scattering angle for a mixture of dilute (ideal) species is given by Stacey [7]

$$R(0, \{w\}) = K' \sum_i \left(\frac{dn}{dw_i} \right)^2 M_i w_i, \quad (2)$$

where w_i and dn/dw_i denote, respectively, the weight/volume concentration and the specific refractive increment of the i th solute species. If, in addition, all scattering species have the same chemical composition (e.g., a polymer with a distribution of chain length or a single protein that self-associates to form different oligomeric species) then the refractive increment of all species is equal, and Eq. (2) simplifies to

$$R(0, w_{\text{tot}}) = K \sum_i M_i w_i = K w_{\text{tot}} M_W, \quad (3)$$

where $K \equiv K' (dn/dw)^2$, w_{tot} is the total concentration of solute, and M_W is the weight-average molar mass.

The dependence of $R(0, w_{\text{tot}})$ upon w_{tot} is obtained as follows. The data points—typically several thousand—are tabulated as a function of two variables, w_{tot} and $\sin^2(\theta/2)$. A two-dimensional polynomial of the form

$$Z(\theta, w_{\text{tot}}) \equiv \frac{R(\theta, W_{\text{tot}})}{K} = \sum_{i=0}^{j_{\text{max}}} \sum_{j=1}^{j_{\text{max}}} C_{ij} [\sin^2(\theta/2)]^i w_{\text{tot}}^j \quad (4)$$

is fit globally to the entire data set by linear least squares. Combination of Eqs. (3) and (4) yields

$$M_W = \frac{Z(0, w_{\text{tot}})}{w_{\text{tot}}} = \sum_{j=1}^{j_{\text{max}}} C_{0j} w_{\text{tot}}^{j-1}. \quad (5)$$

The Fisher F test [17] is used to determine the minimum values of i_{max} and j_{max} permitting Eq. (4) to describe the entire data set to within experimental uncertainty. Glob-

ular proteins whose maximum dimension is less than 1/20th of the wavelength of scattering light (ca. 35 nm) should behave as point particles with no angular dependence of scattering [7]. For these solutes a lowest acceptable value of $i_{\max} > 0$ is indicative of either an instrumental artifact or the presence of aggregates formed subsequent to prefiltration of the protein stock solution.

If the data are described to within experimental precision by Eq. (4) with $i_{\max} = 0$, $j_{\max} = 1$, then M_W is independent of concentration over the range of solute concentrations up to that of the stock solution. This result is consistent with one of two possibilities. (1) There exists a single non-self-interacting solute species, with molar mass M equal to $M_W (= C_{01})$. (2) There exists a mixture of noninteracting solute species. One cannot discriminate between these two possibilities on the basis of a single experiment conducted as described in the previous section, since a distribution of species (and M_W) would not be altered by simple dilution. However, the presence of multiple solute species may be revealed by size exclusion chromatography, native gel electrophoresis, and/or sedimentation velocity experiments.

If a satisfactory description of the data according to Eq. (4) requires C_{02} to be significantly greater than 0 (i.e., M_W increasing with solute concentration), then the presence of equilibrium association is indicated. Conversely, if a satisfactory description of the data according to Eq. (4) requires C_{02} to be significantly less than 0 (i.e., M_W decreasing with solute concentration), then the solution is exhibiting nonideal behavior arising from repulsive solute–solute interaction [7]. In the present work we shall consider only self-association of a single ideal solute component and defer consideration of multicomponent and/or nonideal solutions to later papers in this series.

Characterization of equilibrium self-association

When the multiangle scattering data may be satisfactorily described by Eq. (4) with $i_{\max} = 0$, indicating a lack of angular dependence, a further simplification is possible. For each time (or concentration) point, the values of $Z (= R/K)$ obtained at 15 scattering angles are averaged, and the results are saved as a table of $\{w_{\text{tot}}, \langle Z \rangle(w_{\text{tot}})\}$. This process is referred to as “data condensation.” The dependence of $\langle Z \rangle$ upon w_{tot} is then modeled in the context of a model for equilibrium self-association as indicated below.

Consider a monomeric protein A in equilibrium with one or more oligomeric species A_i . The (equilibrium) molar concentration of each i -mer is given by

$$c_i = K_i c_1^i, \quad (6)$$

where c_i denotes the molar concentration of i -mer. Conservation of mass is expressed as

$$c_{\text{tot}} = w_{\text{tot}}/M_1 = \sum c_i = \sum iK_i c_1^i. \quad (7)$$

Eq. (7) may be solved analytically or numerically for c_1 as a function of w_{tot} , M_1 , and the various K_i . Then each of the c_i may be calculated using Eq. (6), and it follows from Eq. (5) that:

$$Z = M_W w_{\text{tot}}, \quad (8a)$$

where

$$M_W = \frac{\sum M_i w_i}{\sum w_i} = M_1 \frac{\sum i^2 c_i}{\sum i c_i}. \quad (8b)$$

The values of M_1 and each K_i (or preferably $\log_{10} K_i$) are estimated by nonlinear least-squares fitting of Eqs. (6)–(8) to the experimentally measured dependence of $\langle Z \rangle$ upon w_{tot} .

Results

Nonassociating proteins

The results of analysis of data obtained for ovalbumin (data shown in Fig. 2) are plotted for different stages of refinement in Figs. 3A and B. The raw data set consists of 16,755 values of Z , which are plotted as a function of w_{tot} and $\sin^2(\theta/2)$ in the left panel of Fig. 3A. Also plotted is the best fit of Eq. (4) with $i_{\max} = 0$, $j_{\max} = 1$, and $C_{01} = 44,388 \pm 22$ (95% confidence limits). The corresponding best-fit residuals are plotted in the right panel of Fig. 3A. The left and right panels of Fig. 3B show the results of the same analysis applied to a filtered subset of the initial data set, obtained by deleting all of the points in the original data set with values of the squared best fit residual greater than three times the value of the mean squared best-fit residual. This subset has 16,696 data points, and the best-fit value of $C_{01} = 44,341 \pm 8$. It may be seen that the filtering procedure does not significantly alter the result of the analysis, indicating that the small number of outliers in the raw data set have no significant effect on the determination of the molar mass. In Fig. 4, the value of $\log M$ determined for several proteins by the method described above is plotted against the value of $\log M$ for the corresponding protein obtained from the literature.

Self-associating proteins

Some of the proteins examined exhibited a significant improvement in the quality of fit of Eq. (4), as measured by the magnitude of the sum of squared residuals, when j_{\max} was increased from 1 to 2, and best-fit values of C_{02} were found to be significantly greater than zero. A further increase of j_{\max} from 2 to 3 did not result in further significant lowering of the sum of squared residuals. These data sets were then condensed as described above.

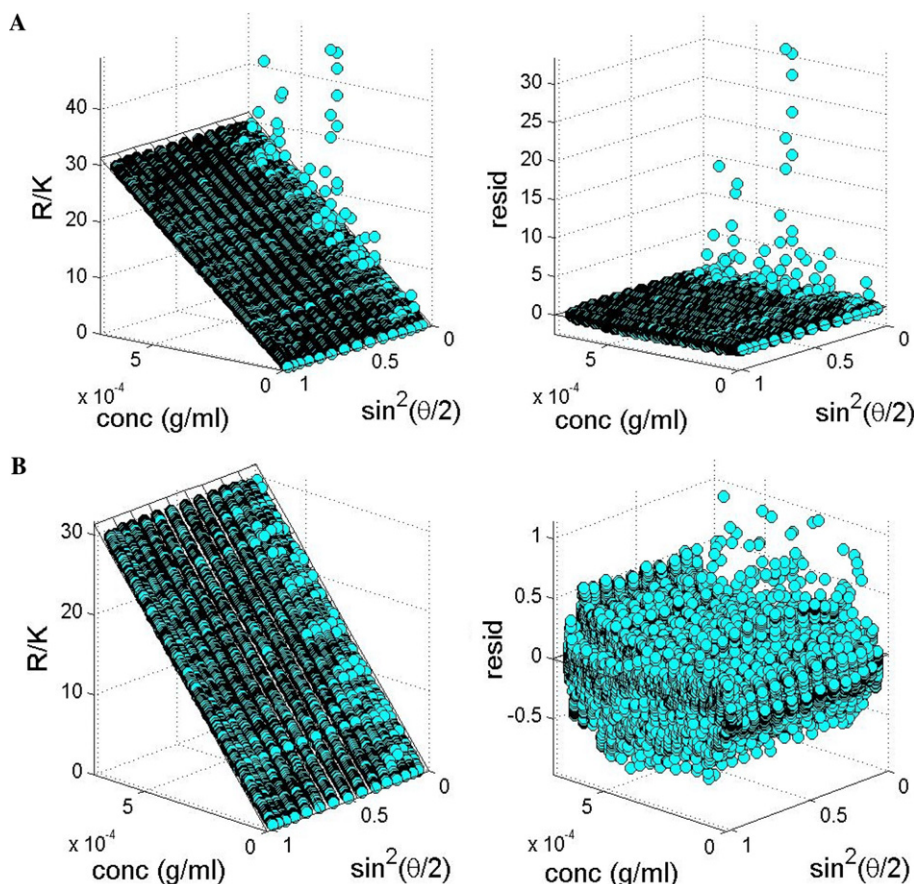


Fig. 3. Stages in processing data obtained from the experiment shown in Fig. 2. In each panel, the lefthand plot indicates experimentally obtained values of R/K (symbols) and the best fit of Eq. (4) with $i_{\max} = 0$, $j_{\max} = 1$ (grid lines), plotted as a function of concentration and $\sin^2(\theta/2)$. The righthand plot indicates the difference between experimental and calculated best-fit values of R/K , plotted against the same coordinates. (A) Unfiltered data; (B) data filtered as described in text.

Ideal monomer–dimer self-association models based upon Eqs. (6)–(8) were fit to the condensed data sets by the method of nonlinear least squares to obtain best-fit estimates of M_1 and $\log K_2$ (M^{-1}). Experimentally measured values of $\langle R \rangle / K$ for β -lactoglobulin are plotted as a function of w_{tot} in Fig. 5, together with the best fit of a monomer–dimer equilibrium association model. Best-fit parameter values for this and other self-associating proteins are summarized in Table 1.

Discussion

The measurement and analysis of excess static light scattering of macromolecules in solution has traditionally been carried out in batch mode. A series of solutions containing a macrosolute at different concentrations is prepared and then, in sequence, each solution is introduced into the scattering cell and the scattering is measured at multiple angles. For each solute concentration, an apparent weight-average molar mass and, for sufficiently large macrosolutes, the z -average radius of

gyration of the solute are determined by linear regression of $R(\theta, w_{\text{tot}}) / Kw_{\text{tot}}$ or $Kw_{\text{tot}} / R(\theta, w_{\text{tot}})$ [6,7]. The presence of significant solute–solute interaction under a particular set of experimental conditions is manifested as a concentration dependence of the apparent weight-average molar mass [14,18,19].

The experimental and analytical methods introduced here improve on the traditional approach described above in several respects. (1) The total amount of macrosolute required for the complete analysis is many times smaller. (2) A more complete characterization of concentration dependence of solution properties is achieved via a continuous gradient of concentration in contrast to a few discrete concentrations. (3) The process of data acquisition is much more rapid. (4) Attempts to model values of $R(0, w_{\text{tot}}) / Kw_{\text{tot}}$ or $Kw_{\text{tot}} / R(0, w_{\text{tot}})$, which are themselves obtained by regression, as functions of the independent variable w_{tot} are problematic both statistically and numerically. These variables, which are conventionally treated in the context of regression as nominally dependent variables, are not dependent variables but rather extremely complex

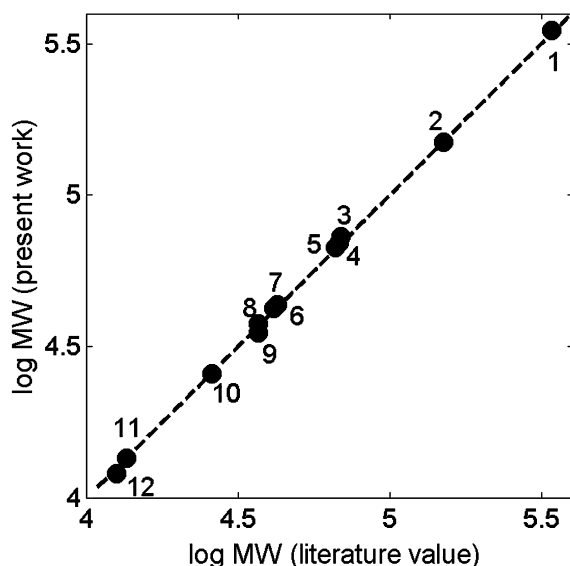


Fig. 4. Logarithm of molar mass obtained for various proteins by the procedure described here, plotted against the logarithm of molar mass for the same proteins obtained from the literature. Dashed line indicates equal-valued x and y coordinates. Proteins are listed together with references to published values of the molar mass: (1) fibrinogen [26], (2) alcohol dehydrogenase [26], (3) bovine serum albumin [nonequilibrium mixture of monomer + oligomers] [27], (4) hemoglobin, (5) bovine serum albumin [monomer] [28], (6) ovalbumin [26], (7) pepsinogen [29], (8) β -lactoglobulin [mixture of A and B] [30], (9) β -lactoglobulin A [20], (10) chymotrypsinogen A [18], (11) lysozyme [26], and (12) cytochrome c [26].

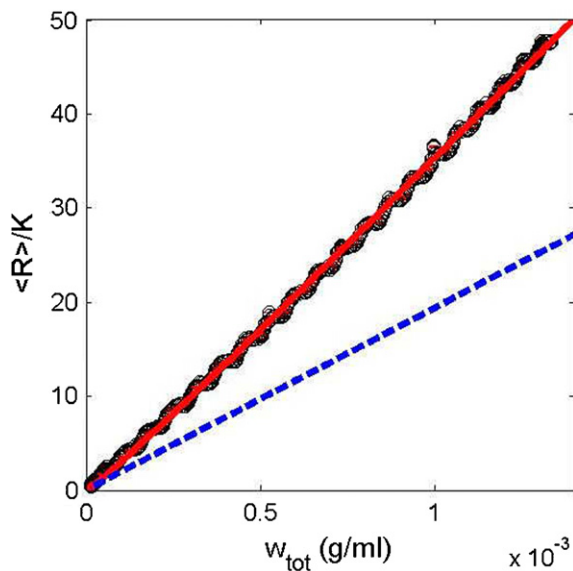


Fig. 5. $\langle R \rangle / K$ plotted as a function of w_{tot} for β -lactoglobulin. Points, experimental data: red solid line, best fit of monomer–dimer model, calculated with best-fit parameter values shown in Table 1; blue dashed line, hypothetical dependence of $\langle R \rangle / K$ upon w_{tot} in the absence of self-association, calculated using best-fit monomer molecular weight. (For interpretation of the references to color in this figure legend, the reader is referred to the web version of this paper.)

compound variables; moreover, the precision of either variable diverges in the sought limit of low concentration. In contrast, in the present analysis, the concentration dependence of zero-angle scattering is obtained via robust and essentially instantaneous global modeling of $R(\theta, w_{tot})/K$ at all scattering angles and all concentrations, with no loss of precision beyond that inherent in the signal/noise ratio of the raw data at low concentrations.

Previous investigations of the behavior of β -lactoglobulin [20] and chymotrypsinogen A [18] have established that these proteins do self-associate under conditions comparable to those of the present experiments, but a quantitative comparison between earlier and present results is not possible due to significant differences in temperature, ionic strength, and/or buffer composition. However, equilibrium constants for dimer–tetramer association of oxy- and carboxyhemoglobin, measured previously under conditions almost identical to those employed here, have been tabulated [21: Tables 5.11 and 5.12]. Since cyanmet-, oxy-, and carboxyhemoglobin share the same quaternary structure [22], their dissociation behavior is expected to be similar. As shown in Fig. 6, values of the equilibrium association constant of cyanmethemoglobin obtained in the present work agree with the tabulated values for oxy- and carboxyhemoglobin to within experimental uncertainty at all three values of the ionic strength.

The analysis of equilibrium self-association presented here is based upon the assumption that equilibration between the various associating species is rapid with respect to the rate of change of composition of the solution. To check the validity of this assumption, a delay time was introduced following the addition of successive increments of solution, and the scattering versus time curve was examined for the appearance of relaxations that are significantly slower than the mixing time as monitored by the rate of change of absorbance. In this manner we observed a significant scattering lag accompanying the addition of large quantities of buffer to small quantities of stock β -lactoglobulin, which was attributed to the time required for protein association to reequilibrate following rapid dilution. A corresponding lag was not observed in the downward gradient of concentration, where dilution is gradual rather than abrupt. We therefore subsequently analyzed only descending gradients of concentration in the self-associating protein systems and, for each protein studied, performed experiments at different rates of concentration change to ascertain that the derived dependence of $\langle R \rangle / K$ upon total concentration was independent of this rate.

There is a close analogy, both thermodynamic and methodological, between the present approach to measurement and analysis of light scattering and the measurement and analysis of sedimentation equilibrium.

Table 1
Results of modeling light scattering data in the context of a model for ideal monomer–dimer equilibrium self-association

Protein	Number of data sets	M_1 (best-fit)	$\log K_2$ (M^{-1}) (best-fit)
β -Lactoglobulin	3	19,600 [18,800; 20,500]	5.3 [5.0; 5.7]
Chymotrypsinogen	2	23,600 [23,100; 24,000]	3.25 [3.1; 3.35]
Cyanmethemoglobin [NaCl] = 0.15 M	1	35,700 ^a [33,900; 38,000]	5.8 [5.2; 7.1]
Cyanmethemoglobin [NaCl] = 1 M	2	32,200 ^a [29,500; 37,000]	4.7 [4.1; 5.2]
Cyanmethemoglobin [NaCl] = 2 M	2	33,400 ^a [29,500; 37,000]	4.1 [3.8; 4.5]

Bracketed values following best-fit values represent lower and upper 95% confidence limits of estimate.

^a The association process characterized corresponds to $2(\alpha\beta) \rightleftharpoons \alpha_2\beta_2$.

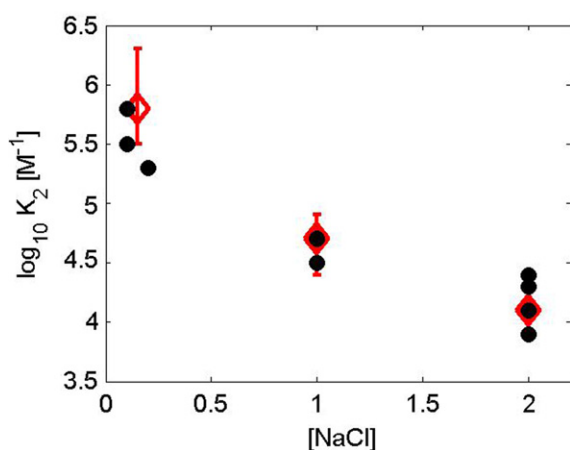


Fig. 6. Comparison of equilibrium constants for the association of cyanmethemoglobin half-molecules determined at several ionic strengths in the present work (diamonds) and association of carboxy- and oxyhemoglobin in previous studies (circles), as tabulated in Antonini and Brunori [21]. Error bars correspond to 95% confidence limits of estimate.

In the light scattering experiment, one simultaneously measures concentration and total solute scattering, a property that depends upon the product of solute mass and refractive increment of each solute species and upon the interactions, both attractive and repulsive, between solute molecules [7,12]. In the centrifugation experiment, one simultaneously measures concentration and the equilibrium gradient of solute(s), a property that depends upon the product of solute mass and density increment of each solute species and upon the interactions, both attractive and repulsive, between solute molecules [23–25]. In both types of experiment, information about solute–solute interactions is obtained from observed differences between the measured property of the solution and the expected sum of the properties of isolated (noninteracting) solutes. Our goal is to acquire information about reversible associations that is comparable in scope and resolution to that currently obtainable from sedimentation equilibrium. Since the

methodology introduced here, in contrast to that of sedimentation equilibrium, permits extremely rapid acquisition and analysis of composition-dependent data, it may in principle be used to characterize reversible associations evolving with time and at equilibrium and, with the addition of sample handling robotics, may be utilized in moderately high-throughput assays for reversible macromolecular association.

Acknowledgment

This research was supported in part by an appointment (A.K.A.) to the National Institute of Diabetes, Digestive, and Kidney Diseases Research Participation Program, administered by the Oak Ridge Institute for Science and Education.

References

- [1] E.M. Phizicky, S. Fields, Protein–protein interactions: methods for detection and analysis, *Microbiol. Rev.* 59 (1995) 94–123.
- [2] P.A. Srere (Ed.), Special Issue: Heterologous Protein–Protein Interactions, *Methods* 19 (1999) 191–349.
- [3] C. von Mering, R. Krause, B. Snel, M. Cornell, S.G. Oliver, S. Fields, P. Bork, Comparative assessment of large-scale data sets of protein–protein interactions, *Nature* 417 (2002) 399–403.
- [4] P. Debye, Molecular weight determination by light scattering, *J. Phys. Coll. Chem.* 51 (1947) 18–32.
- [5] B.H. Zimm, The scattering of light and the radial distribution function of high polymer solutions, *J. Chem. Phys.* 16 (1948) 1093–1099.
- [6] B.H. Zimm, Apparatus and methods for measurement and interpretation of the angular variation of light scattering: preliminary results on polystyrene solutions, *J. Chem. Phys.* 16 (1948) 1099–1116.
- [7] K.A. Stacey, *Light-Scattering in Physical Chemistry*, Academic Press, New York, 1956.
- [8] L. Jeng, S.T. Balke, T.H. Mourey, L. Wheeler, P. Romeo, Evaluation of light scattering detectors for size-exclusion chromatography 1. Instrument precision and accuracy, *J. Appl. Polym. Sci.* 49 (1993) 1359–1374.

- [9] L. Jeng, S.T. Balke, Evaluation of light scattering detectors for size-exclusion chromatography 2. Light scattering equation selection, *J. Appl. Polym. Sci.* 49 (1993) 1375–1385.
- [10] J. Wen, T. Arakawa, J.S. Philo, Size-exclusion chromatography with on-line light-scattering, absorbance and refractive index detectors for studying proteins and their interactions, *Anal. Biochem.* 240 (1996) 155–166.
- [11] B.S. Kendrick, B.A. Kerwin, B.S. Chang, J.S. Philo, Online size-exclusion high-performance liquid chromatography light scattering and differential refractometry methods to determine degree of polymer conjugation to proteins and protein–protein or protein–ligand association states, *Anal. Biochem.* 299 (2001) 136–146.
- [12] W.H. Stockmayer, Light scattering in multi-component systems, *J. Chem. Phys.* 18 (1950) 58–61.
- [13] R.F. Steiner, Reversible association processes of globular proteins. I. Insulin, *Arch. Biochem. Biophys.* 39 (1952) 333–354.
- [14] H. Tojo, K. Horiike, K. Shiga, Y. Nishina, H. Watari, T. Yamano, Self-association mode of a flavoenzyme: D-amino acid oxidase from hog kidney. Analysis of apparent weight-average molecular weight data for the apoenzyme in terms of models, *J. Biol. Chem.* 260 (1985) 12607–12614.
- [15] R.E. Benesch, R. Benesch, R. Edalji, C. Kwong, Intermolecular effects in the polymerization of hemoglobin S, *Biochem. Biophys. Res. Commun.* 81 (1978) 1307–1312.
- [16] G.E. Perlmann, L.G. Longworth, The specific refractive increment of some purified proteins, *J. Am. Chem. Soc.* 70 (1948) 2719–2724.
- [17] W.H. Press, B.P. Flannery, S.A. Teukolsky, W.T. Vetterling, *Numerical Recipes: The Art of Scientific Computing*, Cambridge University Press, Cambridge, 1987.
- [18] J. Osborne, R.F. Steiner, The self-association of chymotrypsinogen, *Arch. Biochem. Biophys.* 152 (1972) 849–855.
- [19] T. Yamaguchi, K. Adachi, Hemoglobin equilibrium analysis by the multiangle laser light-scattering method, *Biochem. Biophys. Res. Commun.* 290 (2002) 1382–1387.
- [20] M.J. Kelly, F.J. Reithel, A thermodynamic analysis of the monomer–dimer association of β -lactoglobulin A at the isoelectric point, *Biochemistry* 10 (1971) 2639–2644.
- [21] E. Antonini, M. Brunori, Hemoglobin and Myoglobin in their Reactions with Ligands, North-Holland, Amsterdam, 1971.
- [22] M.C. Marden, L. Kiger, J. Kister, B. Bohn, C. Poyart, Coupling of ferric iron spin and allosteric equilibrium in hemoglobin, *Biophys. J.* 60 (1991) 770–776.
- [23] D. Winzor, M. Jacobsen, P. Wills, Direct analysis of sedimentation equilibrium distributions reflecting complex formation between dissimilar reactants, *Biochemistry* 37 (1998) 2226–2233.
- [24] P. Wills, M. Jacobsen, D. Winzor, Analysis of sedimentation equilibrium distributions reflecting nonideal macromolecular associations, *Biophys. J.* 79 (2000) 2178–2187.
- [25] S. Zorrilla, M. Jiménez, P. Lillo, G. Rivas, A.P. Minton, Sedimentation equilibrium in a solution containing an arbitrary number of solute species at arbitrary concentrations: theory and application to concentrated solutions of ribonuclease, *Biophys. Chem.* 108 (2004) 89–100.
- [26] G.D. Fasman (Ed.), *Handbook of Biochemistry and Molecular Biology, Proteins*, vol. II, CRC Press, Cleveland, 1976.
- [27] S.M. Klainer, G. Kegeles, Simultaneous determination of molecular weights and sedimentation constant, *J. Phys. Chem.* 59 (1955) 952–955.
- [28] J.T. Yang, The viscosity of macromolecules in relation to molecular conformation, *Adv. Protein Chem.* 16 (1961) 323–400.
- [29] R.C. Williams, T.G. Rajagopalan, Ultracentrifugal characterization of pepsin and pepsinogen, *J. Biol. Chem.* 241 (1966) 4951–4954.
- [30] K.A. Piez, E.W. Davie, J.E. Folk, J.A. Gladner, Beta-lactoglobulins A and B, *J. Biol. Chem.* 236 (1961) 2912–2916.